Cold gas in distant galaxies

Boogaard, L.A.

1 | Introduction

Abstract

The formation and evolution of galaxies is fundamentally driven by the formation of new stars out of cold gas. Observations of young stars in distant galaxies in the early universe, such as we can see in the *Hubble* Ultra Deep Field, have unveiled how the cosmic star formation rate density evolves. Yet, while the *effect* of star formation—the young stars—has been mapped in ever-increasing detail, the *cause*—the cold molecular gas that fuels star formation—has been elusive. This thesis presents an observational study of the cold interstellar medium of distant galaxies in the early universe, using the most sensitive submillimeter telescope to date, the *Atacama Large Millimeter Array*, together with new integral-field spectrographs, such as the *Multi Unit Spectroscopic Explorer* on the *Very Large Telescope*. It unveils the physical properties of star-forming galaxies and their molecular gas reservoirs, and describes the evolution of the cosmic molecular gas density—*the fuel for star formation*.

1.1 From effect to cause

Since the discovery that our home galaxy, the Milky Way, and other galaxies are separate islands of stars in the universe, and their earliest classifications into spirals and ellipticals (Hubble, 1926), it has become clear that galaxies can be broadly subdivided into two categories: galaxies with large amounts of gas, and galaxies with little gas. The gas-rich galaxies often appear disk-like or irregular, with lanes of dust obscuring their starlight, hosting young and blue stars, and are actively *star-forming*. The gas-poor galaxies host older and redder stellar populations and appear as *quiescent* spheroids of stars. One of the primary goals of modern day astronomy is to explain how this beautifully varied galaxy population has formed and evolved over time.

The gas and dust that fills the space between the stars is aptly described as the *interstellar medium* (ISM). The gas consists mostly of hydrogen and helium, that is enriched with heavier elements formed by nuclear fusion in the centres of stars. It can cool, or be heated by the stars and the supermassive black hole that lies at the centre of most galaxies, and cycle through different phases where it is in equilibrium: the molecular medium (H_2), the neutral medium (H I), and the ionised medium (H II). Galaxies grow through the formation of new stars, which are born in the cold and dense molecular gas, as it collapses under the influence of gravity. Evidently, a central role in the process of galaxy formation and evolution is played by the cold molecular gas, *the fuel for star formation*.

The processes involved in the formation and evolution of a single galaxy take millions or even billions of years and therefore cannot be observed directly by humankind. Instead, the evolution of galaxies is studied by observing the population at different epochs in the past, tracing the evolution of galaxies through time in a statistical manner. This is possible because light emitted by more distant galaxies takes a longer time to reach our telescopes, because it cannot travel faster than the finite speed of light.[1] The distant galaxies we see today therefore appear to us the way they were when the universe was much younger. The fabric of space and time itself is not static either. It is distorted by the objects that reside within it (gravity; as described by the theory of general relativity) and expands at an accelerating rate. The expansion of the universe shifts the wavelength of a photon that travels towards an observer by a factor $1 + z$, where z is called the *redshift*.[2] The redshift of distant galaxies is therefore a measurement of their distance and the age of the universe at the time of emission.

Arguably the most beautiful and distant views into the past have been obtained by the *Hubble Space Telescope*, through its deep field campaigns in northern, southern and equatorial regions of the sky (Williams et al., 1996; Casertano et al., 2000; Beckwith et al., 2006). The *Hubble* Ultra Deep Field (HUDF), shown in Figure 1.1, is the latest installment and reveals a universe that is filled with galaxies. The most distant galaxies in this image emitted their light when the universe was only a few hundred million years old. They reveal a past galaxy

[1] 299 792 458 m s^{-1} (BIPM, 2019), denoted by c.

[2] $1 + z = a(t_{\rm obs})/a(t_{\rm emit}) = \lambda_{\rm obs}/\lambda_{\rm emit}$, where $a(t)$ is the scale factor of the expansion at the cosmic time, t, of emission (emit) and observation (obs). The name redshift originates from the fact that, for a distant source, the observed wavelength, $\lambda_{\rm obs}$, is greater than the emitted wavelength, $\lambda_{\rm emit}$, and the light therefore appears redder. The relation holds inversely for frequencies, $\nu = c/\lambda$. Note the present day universe corresponds to $z = 0$, whereas higher redshifts refer to progressively earlier times in cosmic history, in a non-linear fashion.

Figure 1.1: A zoom-in on the *Hubble* Ultra Deep Field (HUDF). There are more than 5000 galaxies visible in the image. Some galaxies are so far away that their light, seen in this image, was emitted only a few hundred million years after the big bang. The width of the image on sky is about the same as that of a tennis ball seen across a football field. *Technical details: North points 50° counterclockwise from the top and the image extends 2.′3 × 2.′0 on sky. The total exposure time is about 22.5 days (2 million seconds); see Illingworth et al. (2013). The observations in different filters are combined to an RGB image as follows. Blue: F435W + F606W; Green: F775W + F814W + F850LP; Red: F105W + F125W + F160W. Credit: NASA, ESA, G. Illingworth, D. Magee, P. Oesch, R. Bouwens, and the HUDF09 Team.*

population that looks both remarkably similar and very different from the one we see today. The light seen by *Hubble* has been emitted by the stars and hot gas in distant galaxies, and can be used to trace the formation of new stars and the build-up of their stellar content over cosmic time. These images also testify to the common assumption in cosmology that the universe is spatially homogeneous and isotropic,[3] which allows us to make inferences about

[3]While the individual galaxies are different in each image, the universe, when averaged over large enough volumes, looks the essentially same in all directions and earth is in no special place (that is, in a spatial sense; temporally speaking, it is a interesting fact that humankind exists on earth at this specific cosmic time).

galaxy evolution.

Surveys across the electromagnetic spectrum and large computer simulations have greatly advanced our understanding of the formation and evolution of the galaxy population throughout cosmic time. A fundamental aspect of galaxy formation and evolution is to understand where, when and how the stars in galaxies have formed. The *effect* of star formation, the rate at which galaxies form new stars and the build-up of their stellar mass, has been mapped in distant galaxies in ever-increasing detail. In contrast, our knowledge of the *cause*, the cold gas that fuels the star formation, has remained limited, as it difficult to measure in distant galaxies. This has now changed, through advances that have been made in astronomical instrumentation in the last decade. In this thesis, we use these novel instruments to study of the cold gas in distant galaxies, and its implication for our understanding of galaxy formation.

The questions that are central to this thesis are: How does the cold molecular interstellar medium of galaxies evolve over cosmic time, in relation to their star-forming properties, and how does this dictate their evolution? How do galaxies cycle gaseous material in and out of their interstellar medium, driving their evolution over cosmic time?

1.2 The theory

Galaxy formation and evolution is a complex phenomenon that involves processes operating over a vast range of scales in both space and time. On one hand, the formation of stars itself takes place deep inside the cold ISM of galaxies, on scales that are much smaller than the size of a single galaxy. On the other hand, it relies on the potential of fueling star formation over time, through the accretion and cooling of gas from large distances, on scales much larger the size of a single galaxy. The formation and evolution of a galaxy therefore cannot be viewed independently from its place in the universe and the cosmological context in which it evolves.

1.2.1 Cosmology, galaxy formation and the baryon cycle

The current best description of the content of the universe is contained in what is called the concordance model of cosmology; the Λ cold dark matter (ΛCDM) paradigm. Here Λ is the cosmological constant originally defined by Einstein (1917), that describes the accelerated expansion of the universe (Riess et al., 1998; Perlmutter et al., 1999). We observe the universe through the light emitted by the ordinary baryonic[4] matter, which can interact with electromagnetic radiation. However, the baryonic matter alone is insufficient to explain the gravity of, for example, (clusters of) galaxies. This has lead to the postulation of *dark matter* (that does not, or extremely weakly, interact via electromagnetic radiation), which has been a very successful paradigm to explain the dynamic nature of the anomalous gravity in the universe. According to recent measurements, the universe consists of about 5% baryonic matter and 26% dark matter, while the cosmological constant (due to its unknown nature also referred to as *dark energy*) contains around 69% of the total energy density (Planck Collaboration et al.,

[4]It is common in cosmology to refer to all visible matter (consisting of protons, neutrons, and electrons) as baryonic, even though the electron is a lepton and not a baryon.

2020). Reversing the cosmological model in time, we infer that the universe is around 13.8 billion years old and started hot and dense in what is known as the *big bang*.

The process of galaxy formation can be traced back to the *Cosmic Microwave Background* (CMB). This afterglow of the hot and dense gas in the early universe, that decoupled once the gas became neutral, still permeates the present day universe (Penzias & Wilson, 1965). Minute variations in the temperature of the CMB are believed to reflect small density fluctuations in the otherwise homogeneous and isotropic gas in the early universe, and as such the initial conditions for galaxy formation. The composition of this primordial gas is set by the nucleosynthesis of elements that occurred after the big bang and almost exclusively consists of hydrogen ($\approx$ 75%) and helium-4 ($\approx$ 25%), with traces of heavier elements at the $\leq$ 0.1% level (e.g., Schramm & Turner, 1998). This epoch where the universe is filled with neutral gas is referred to as the *dark ages* and lasts until the escaping ionising radiation from the first galaxies initiates a global phase-transition back to the ionised state, during what is called the *epoch of reionisation*, which ends when the universe is around 1 billion years old (e.g., Barkana & Loeb, 2001; Loeb & Barkana, 2001).

As the universe expands, the matter inside expands with it, while slightly overdense regions are being pulled together by gravity at the same time. When the density in a region exceeds a certain threshold (around 200 times the background density), it collapses. The dark matter cannot cool radiatively and forms what is known as a dark matter halo. The gas can fall into these halos to form the visible parts of a galaxy. Over time, the dark matter halos, and the galaxies that reside within them, can grow hierarchically through merging (White & Rees, 1978; Blumenthal et al., 1984; White & Frenk, 1991). On the largest scales, gravity shapes these overdensities into the large scale filamentary structure of the universe that is known as the *cosmic web*.

In contrast to the dark matter, the baryonic matter inside a halo can further cool radiatively and neutral gas (H I) can settle in the centre of the potential well. This is where the gas can cool even further to feed the central supermassive black hole,[5] or convert into dense clouds of molecular gas (H_2) that can gravitationally collapse to form stars. This process is central to galaxy formation: as long as cold gas can be supplied and collapse to form stars, galaxies can continue to build up their stellar mass.

In their core, stars fuse the primordial elements into all the heavier elements that we are so familiar with on earth, such as carbon, nitrogen, oxygen, and iron. These elements are returned into the ISM through stellar winds or supernova explosions. As such, the ISM enriches in metals and dust over time and subsequent generations of stars that are born out of more metal rich gas have higher *metallicity*,[6] such as our Sun (Asplund et al., 2009). A significant fraction of these elements are locked into solid-phase dust grains, which play an important role in the heating and cooling of the ISM and the formation of molecules.

During various stages of their evolution, stars and black holes can drive out gas through their ionising radiation, winds, supernovae, or by accretion onto the supermassive black hole

[5] The formation and (co)evolution of the central supermassive black hole (e.g., Kormendy & Ho, 2013) is another important aspect of galaxy evolution, that we will not focus on here.

[6] In astronomy, all elements more massive than hydrogen and helium (the two elements that together make up $>$ 99% of the cosmic mass budget) are collectively referred to as metals. The mass fraction of these metals in a particular environment is called its metallicity.

(giving rise to an active galactic nucleus; AGN). This *feedback* can suppress or completely halt the gas accretion, blowing gas from the ISM back into the circumgalactic medium, or even out of the halo into the intergalactic medium. These processes may quench the star formation in galaxies temporarily or even permanently. The process where the matter in the universe is heated and cooled and transfers through the various phases (molecular, neutral, ionised, and in-and-out-of stars) both in- and outside galaxies is called the *baryon cycle* (e.g., Tumlinson et al., 2017; Péroux & Howk, 2020). One particularly relevant aspect of the baryon cycle is to understand what fraction of the gas was situated in-and-around galaxies, and available for the formation of stars through cosmic time (e.g., Walter et al., 2020).

It should be mentioned that our understanding of the process of galaxy formation, as outlined above, is greatly aided by numerical simulations on supercomputers. These can compute the evolution of astronomical systems through cosmic time, from single stars and molecular clouds, to galaxies, and even complete universes (including dark and/or baryonic matter). Modern and large cosmological hydrodynamic simulations (e.g., Schaye et al., 2015; Crain et al., 2015; Pillepich et al., 2018; Nelson et al., 2018) include many physical processes and provide an accurate description of a wide range of galaxy properties. Truly *ab initio* cosmological simulations of galaxy formation are still beyond the capabilities of modern computational facilities, however, due to the vast range of spatial scales involved (see Somerville & Davé 2015 and Naab & Ostriker 2017 for recent reviews). They typically rely on subgrid physics to describe the processes that happen below the resolution limit with preset (tunable) parameters, such as star formation (that is, the efficiency with which gas is converted to stars, as they generally do not resolve the cold ISM) and the strength of feedback (e.g., Schaye et al., 2010). A different approach is taken by semi-analytical models, that do not solve the fundamental physical equations at certain resolution, but instead use equations to describe the flow of bulk material between different phases. Studies of the cold ISM in cosmological simulations typically resort to refining the simulated gas into the different cold phases during post-processing of cosmological simulations, or by using semi-analytical models (e.g., Popping et al., 2019). Testing and breaking these (and future) simulations with improved observations is important to forward our understanding of the physical processes involved. Conversely, the predictions from simulations are a valuable tool to understand the limitations and improve the design of observations.

1.2.2 Star formation and the cold interstellar medium

In the Milky Way and other galaxies, star formation takes place inside *Giant Molecular Clouds* (GMCs) of cold ($T = 10 - 50$ K) and dense gas ($n_{\rm H} \geq 10^3$ cm^{-3}) with sizes ranging from a few parsec[7] up to roughly 100 pc (e.g., Solomon et al., 1987; McKee & Ostriker, 2007; Bolatto et al., 2008).[8, 9] These GMCs fragment into clumps and cores and are the birthplace of populations of stars. The detailed physics of this process is a field of study on its own and we will not

[7] A parsec (pc) is a measure of distance and equals about 3.262 light years or 30.86 trillion (10^{12}) kilometres.

[8] A possible exception being the first generation of stars.

[9] Giant Molecular Clouds can be part of larger (gravitationally bound) 'complexes' while individual clouds can fragment into 'cores' and 'clumps'. While individual GMCs often have reasonably well-defined boundaries, there is no universal definition of this delineation. These numbers should therefore be taken as indicative, see Draine (2011).

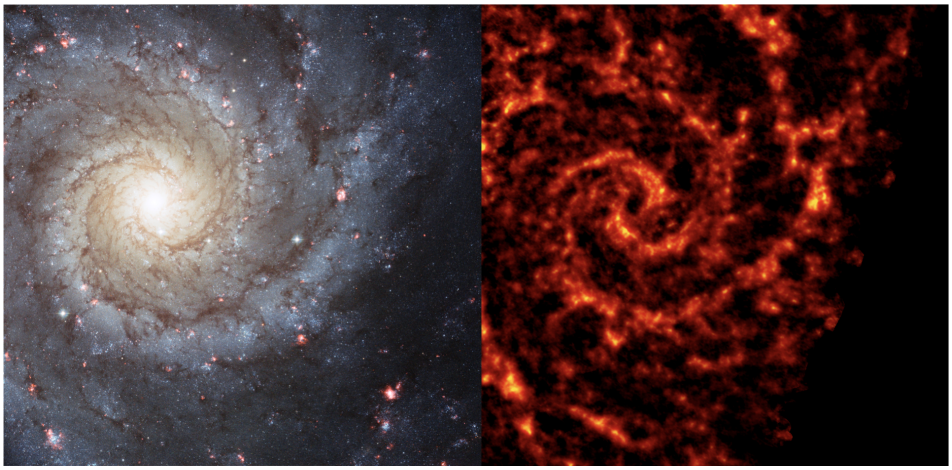

Figure 1.2: The spiral galaxy Messier 74 (NGC 628) lies at distance of about 10 Mpc. The images show a zoom-in of the face of the disk of about 10 kpc on each side. The *Hubble* image (*left*) shows the starlight, that appears bluer in the spiral arms and redder towards the nucleus. Lanes of dust obscuring the starlight appear as filamentary brown structures. The bright red spots show emission from ionised hydrogen in the H II regions around recently formed stars. The ALMA image (*right*) shows the cold molecular gas in giant molecular clouds, as traced by emission from carbon monoxide, at 50 pc resolution. The cold molecular gas is coincident with the dust and the spiral arms where new stars are formed. *Left: Blue: F435W, Green: F555W, Red: F656N (Hα + [N II]) + F814W. Right: Emission from CO $J = 2 \rightarrow 1$; the black area towards the bottom right of the panel lacks observations. Credits: NASA, ESA, and the Hubble Heritage Collaboration, R. Chandar and J. Miller (left). ALMA (ESO/NAOJ/NRAO), NRAO/AUI/NSF and the PHANGS collaboration, B. Saxton (right).*

concern ourselves with it here (the interested reader can start exploring in, e.g., McKee & Ostriker, 2007). The reason is that the substructure of GMCs has been (and still is) very difficult to resolve in all but the most nearby galaxies. In the context of galaxy formation and evolution, studies have therefore long focused on linking the surface density of star formation and cold (H I and H_2) gas over larger scales (Schmidt, 1959; Kennicutt, 1998b). More detailed observations now show that the star formation rate correlates with the H_2 density over wide range of surface densities, both in regions where H I is absent or the dominant gas component (e.g., Leroy et al., 2008; Bigiel et al., 2008; Schruba et al., 2011; Leroy et al., 2013), while the denser gas may connect even more strongly (e.g., Gao & Solomon, 2004). This supports the long-standing picture that cold molecular H_2 gas is the fuel for star formation in galaxies (e.g., Young & Scoville, 1991). The right panel of Figure 1.2 shows observations of the cold molecular gas in a nearby galaxy, which reach the scale of individual GMCs ($\approx$ 50 pc; Kreckel et al. 2018), that are now possible with state-of-the-art submillimeter interferometers (§ 1.3.2).

Observations in the local universe show that galaxies globally consume their gas at, to first order, similar timescales (e.g., Leroy et al., 2013). However, there is still quite a diversity throughout the larger galaxy population (e.g., Saintonge et al., 2016, 2017). To what extent the 'laws' that guide star formation are universal, and to what extent they apply to, for example,

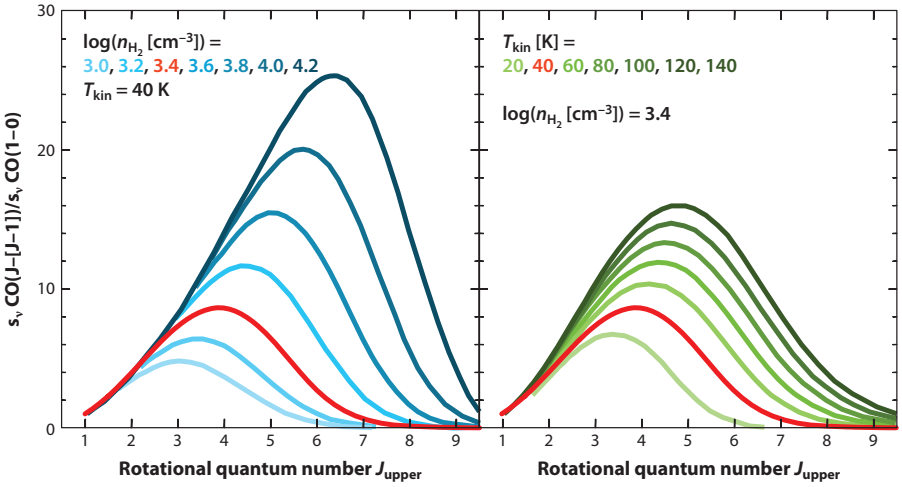

Figure 1.3: Illustration of how the measured CO excitation ladder changes as a function of density and kinetic temperature. *Left:* The effect of changing density at a fixed temperature ($T_{\rm kin} = 40$ K). *Right:* The effect of changing temperature at fixed density ($n_{\rm H_2} = 10^{3.4}$ cm^{-3}). Both panels have been normalised to the CO $J = 1 \rightarrow 0$ transition. High CO excitation is obtained through a combination of high kinetic temperature and high density. *Figure taken from Carilli & Walter (2013).*

starburst galaxies with very high surface densities of gas and star formation, or galaxies with very low metallicities, is a topic of debate (e.g., Kennicutt & Evans, 2012). As the physical conditions in and around galaxies in the distant universe are quite likely different from those in present day galaxies, this raises the question what extent the process of star formation operates in the same fashion, and if not what drives the differences.

Measuring molecular gas

Tracing the mass and distribution of the cold ISM, which consists almost entirely of H_2, is not trivial. Because H_2 is a homonuclear, diatomic molecule, it does not posses a permanent dipole moment with corresponding electric dipole transitions. More importantly, because H_2 is such a low-mass molecule, the lowest energy rotational quadrupole transitions (from the ground state of para- and ortho-H_2) have upper-level energies of $E/k \simeq 510$ K and 1015 K and are not excited inside cold GMCs (and the same is true for the lowest energy vibrational transitions, which require even higher temperatures to excite). As a result, the cold H_2 that makes up most of the ISM is practically invisible in emission (Bolatto et al., 2013).

Trace species must therefore be used to measure the molecular gas mass. The next most abundant element, the helium atom, suffers from similar observability problems as H_2. Fortunately, the cold interstellar medium is also the site where hydrogen and the more abundant elements such as carbon, nitrogen and oxygen, can enter into richer chemistry, forming molecules. Besides molecules, the cold ISM also harbours significant amounts of dust. The dust plays an important role in the chemistry of the ISM, being a catalyst for the

formation of H_2, and can be observed in both absorption and emission.

Carbon monoxide is the most abundant molecule in the cold ISM and $^{12}C^{16}O$ (hereafter, CO) is its most abundant isotopologue. In contrast to H_2, the heteronuclear CO molecule has a weak permanent dipole moment and its rotational transitions (denoted by their rotational quantum number J) have a very low excitation temperature. The upper level energy of the first excited state is $E/k = 5.53$ K, which is easily excited even in cold molecular clouds. The CO $J = 1 \rightarrow 0$ transition lies at $\nu_0 = 115.27$ GHz (or $\lambda_0 = 2.60$ mm) and is easily observable at through a transparent atmospheric window (at $z = 0$). As a result, emission from CO has become the workhorse tracer of molecular gas.

Converting the integrated CO luminosity to a molecular gas mass requires a mass-to-light ratio, known as α_{CO}.[10] The value of α_{CO} is calibrated locally, through independent measurements of the total mass of a molecular cloud from, for example, dust emission or extinction, gamma-ray emission, or the virial theorem (see Bolatto et al., 2013, for a recent review). The value of α_{CO} is dependent on the abundance of CO (related to the metallicity), the density and temperature of the emitting medium, and, because the CO emission is optically thick under most circumstances, the geometry. Even after more than half a century of observations, the value of α_{CO} is an important source of uncertainty in determining gas masses, and knowledge of the physical properties of the system under study are essential to make an informed decision about its value. Averaged over galactic scales, there are average values of α_{CO} that seem to apply within reasonable uncertainties, for certain types of galaxies.

The higher-J rotational transitions of CO (with $J > 1$) are also observable, being relatively closely spaced at J-multiples of ν_0. This excitation 'ladder' of rotational transitions is sensitive to (and can be used to constrain) the density and temperature of the cold ISM, and the radiation field (see Figure 1.3). Conversely, knowledge of the CO excitation is crucial to determine gas masses when only higher-J transitions of CO are observed, in order to convert back to the ground-state transition to which α_{CO} is calibrated. This is particularly common at higher redshifts, as transitions may shift to inaccessible parts of frequency space.

An alternative tracer for the cold gas mass is the thermal continuum emission from dust (e.g., Hildebrand, 1983). The Rayleigh-Jeans tail of the dust blackbody at long-wavelengths is most sensitive to the cold dust grains that contain most of the dust mass (the peak of the dust emission is driven by the temperature of the warm grains, which do not contain most of the mass). Because this tail is optically thin, the emission is directly proportional to the dust mass. Deriving the dust mass requires knowledge of the (mass-weighted) temperature of the cold dust, its composition and size distribution, and the corresponding emissivity as a function of wavelength (e.g., Draine & Li, 2001; Li & Draine, 2001). Furthermore, to convert the dust mass to a gas mass requires knowledge of the gas-to-dust ratio. Because the mass in dust is built up over time (until it reaches an equilibrium between formation and destruction) the gas-to-dust ratio can vary from source to source, and is sensitive to the metallicity of the medium (e.g., Rémy-Ruyer et al., 2014). Again, knowledge of the physical conditions of system under study are key to make justified assumptions, while over galactic scales average

[10] Directly related is the well-known conversion factor X_{CO}, that is, the ratio between the (resolved) CO intensity and the hydrogen column density. In this thesis we will exclusively deal with unresolved observations and therefore α_{CO}. The adopted α_{CO} in this work includes a correction factor for the abundance heavy elements, such that the results refer to the total molecular gas mass (not just the mass in H_2).

values may apply within reasonable uncertainty (e.g. Scoville et al., 2016).

Other species can also potentially be used to trace (different parts) of molecular clouds. However, their emission lines are generally much fainter than those of CO and therefore difficult, if not impossible, to detect in distant galaxies, even with modern instruments (though see chapter 4 and chapter 6 for notable exceptions).

Measuring star formation

Once a stellar population is formed, the ionising radiation from the young, hot, blue stars disperse the birth cloud and give rise to an H II region of ionised gas. These can been seen as knots of bright red emission in the left panel of Figure 1.2. The interface between the ionised and molecular medium is called a photodissociation region (PDR; Hollenbach & Tielens 1999), where through an ionisation- and photodissociation front the gas transitions smoothly back from the ionised, to the neutral, to the molecular phase. Inside the hot H II regions the ionised hydrogen atoms recombine with their electrons giving rise to recombination radiation (through the Lyman, Balmer, Paschen, Brackett, etc., series). Ionised and neutral species of carbon, nitrogen and oxygen atoms are often observed in emission through their (semi-) forbidden lines (for example, [O II] $\lambda\lambda$3727, 3730, [O III] $\lambda\lambda$4960, 5008) and fine structure lines (for example, [C I] λ370 μm, [C II] λ158 μm, [O III] λ88 μm). While more complex molecules can radiate from the colder phases (like CO). Together, the emission lines that arise in the different phases of the gas can be used as a direct and indirect diagnostic for the physical properties of the gas, such as its density, temperature, and metallicity, as well as the radiation field and the (ionising) sources that give rise to it, such as stars or an AGN (e.g., Osterbrock & Ferland, 2006; Draine, 2011).

The hottest stars emit most of the ionising radiation and are very short lived ($\leq$ 10 Myr). The number of massive stars can therefore be converted to a total number of recently formed stars, under the assumption an initial mass function (IMF), which is the stellar mass distribution of a population of newly formed stars (throughout this thesis, we adopt the IMF from Chabrier 2003). This star formation rate (SFR) can be measured either from the direct ultraviolet (UV) radiation of the young hot stars, or indirectly by the way the it affects the ISM (see, e.g., Kennicutt & Evans, 2012). An example of the latter are the recombination lines from hydrogen, which trace the SFR well because their recombination rate is directly proportional to the ionising flux, with limited sensitivity to the density and temperature (and metallicity) of the H II region.

The presence of dust grains along the line of sight can have a strong attenuating effect on UV and optical radiation, which proves a significant complication when inferring (for example) the SFR, and needs to be corrected for (e.g., Charlot & Fall, 2000). At the same time, the absorption increases the temperature of the dust grains, which re-emit the radiation at longer wavelengths, in the infrared (IR) and (sub)millimeter (e.g., Galliano et al., 2018). The emission from (warm) dust (including polycyclic aromatic hydrocarbons; PAHs, Tielens 2008) can therefore also be used as a tracer of star formation, either directly, or in combination with the UV.

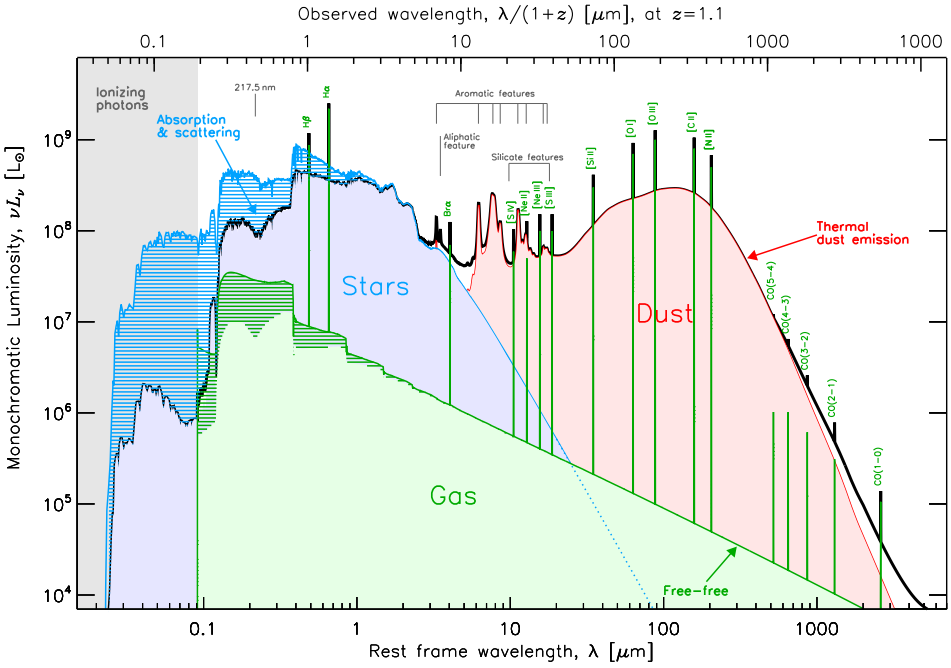

Figure 1.4: An illustration of the spectral energy distribution of a galaxy from the ultraviolet to the millimeter regime. The overall shape (black) is a combination of different components. The emission from stars and gas are show in blue and green, respectively, with the hashed region indicating the fraction of light scattered and absorbed by the dust (which is re-radiated at long-wavelengths). The emission from dust and PAHs (polycyclic aromatic hydrocarbons) is shown in red. Some emission lines from the ionised, neutral and molecular interstellar medium, including several that are relevant to this work, are indicated in green (real galaxies show many more lines that are not shown, for clarity). The top ordinate shows the shift in observed wavelength, for a distant galaxy at $z = 1.1$. *Figure adapted from Galliano et al. (2018), credit: F. Galliano.*

1.2.3 The light from galaxies across the electromagnetic spectrum

A model of the complete *spectral energy distribution* (SED) of a galaxy is shown in Figure 1.4. It emphasises the emission from the stars (at UV, optical and near-IR wavelengths), the emission from the dust (at mid- and far-IR, as well as (sub)millimeter wavelengths), and the emission from the gas (ionised, neutral, and molecular; across the spectrum). The total amount of starlight from galaxies can be modeled to infer the total mass in stars and the techniques to do so have become increasingly sophisticated. Modern approaches aim to describe the overall SED of galaxies across all wavelengths, by modeling the birth and evolution of individual populations of stars over time, including the chemical evolution, and the reprocessing of the light by dust (e.g., Conroy 2013, in some cases also including other phases, such as the ionised gas and associated emission lines). Observations of the colours of galaxies (as measured with broad-band filters with cameras on telescopes, like *Hubble*, cf. Figure 1.1), can be sufficient

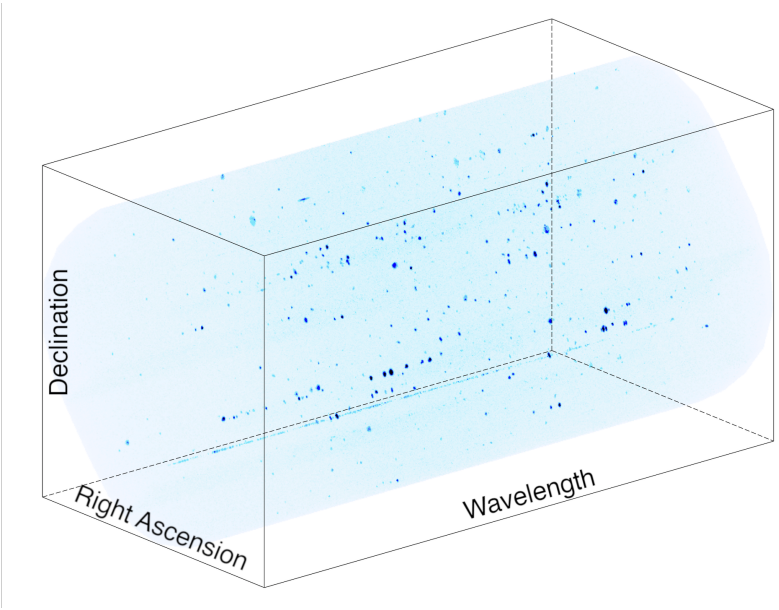

Figure 1.5: Three-dimensional rendering of (part of) the MUSE *Hubble* Ultra Deep Field Survey signal-to-noise cube, that corresponds to the ASPECS field. The (starlight) continuum emission has been subtracted so that the bright emission lines from the hot gas in galaxies are clearly visible as bright spots in the cube. *The rendition uses the 10 h data (Bacon et al., 2017) and spans about 2.′5 in the spatial directions, covering the full wavelength range of MUSE.*

to constrain the overall shape of the SED, from which the total mass in old and young stars can be inferred to within reasonable accuracy. To measure the molecular gas masses and star formation rates from the emission lines (§ 1.2.2), however, requires spectroscopic instruments that break up the light with sufficient resolution, ideally for large numbers of galaxies simultaneously.

1.3 The instruments

Observational astronomy is driven by the development of new telescopes and instruments that improve and expand our view of the sky. Two facilities stand out as being essential to the work presented here and are described in detail below. While both are very different (from a technical point of view) they achieve the same result, that is: to provide spectroscopy for all galaxies within the field of view simultaneously, enabling the study of their properties without any *a priori* target selection. In addition to these two instruments, the work builds on observations of the HUDF taken with a range of instruments, many ground-breaking at the time they became available (and some still are).

1.3.1 Multi Unit Spectroscopic Explorer (MUSE)

The *Multi Unit Spectroscopic Explorer* (MUSE) instrument was installed in 2014 at the Very Large Telescope (VLT) at the European Southern Observatory (ESO) in Paranal, Chile (Bacon et al., 2010; Bacon et al., 2014). MUSE is an optical (4750 – 9300Å), integral-field spectrograph with a square arcminute field of view. It takes an image, but splits the light into a spectrum at every pixel, such that an observation results in a datacube of the sky with wavelength as the third dimension. An example of a MUSE datacube can be seen in Figure 1.5. When observing a deep field with MUSE, the resulting datacube provides a spectrum for every galaxy in the field, that can be used to measure its redshift and infer different physical properties (depending on the redshift).

The HUDF has been extensively observed with MUSE during the Guaranteed Time Observations. The observations consists of a mosaic of 10 h exposures with covering the full field and a single, 30 h exposure in the central region of the field, both taken as part of the MUSE HUDF Survey (Bacon et al., 2017), as well as an ultra-deep series of exposures reaching a total depth of 140 h called the MUSE eXtreme Deep Field (MXDF; R. Bacon, et al., *in prep.*). In total, the MUSE observations provide spectroscopic redshifts for over 10× more galaxies than all previous spectroscopic surveys measured together, which will prove to be essential for the work in this thesis.

1.3.2 Atacama Large Millimeter Array (ALMA)

The *Atacama Large Millimeter/submillimeter Array* (ALMA) started its operations in 2011 and is currently the largest (sub-)millimeter telescope in the world (Wootten & Thompson, 2009). It is a radio-interferometer, consisting of 66 individual antennae operating in different bands that cover the transparent windows in the atmosphere between 84 and 950 GHz (extending down to 35 GHz, once complete). The antennae can be moved around in a variable configuration, from compact (160 m) to extended (16 km), to provide a range from sensitive low-resolution images, to extremely high resolution images. ALMA is the most sensitive telescope to detect emission from in particular the gas and dust in the cold and warm interstellar medium. It is now revolutionising observations of the cold ISM in all facets of astronomy, from the inside of protoplanetary disks around newly forming stars, to the evolution of the cosmic cold molecular gas content of galaxies. The ALMA observations of the HUDF studied in this thesis are presented in § 1.5.

1.3.3 Other facilities

Besides MUSE and ALMA, this thesis builds on the work done by the *Hubble Space Telescope* and other observatories on earth and in space, such as *Chandra* in the X-rays, and *Spitzer* and *Herschel* in the near- and far-IR. The rest-frame optical wavelength regime shifts to the near-IR for galaxies at higher redshift. For the last chapter, we therefore obtained rest-frame optical spectroscopy taken with the *K-band Multi Object Spectrograph* (KMOS) at the VLT and the *Multi-Object Spectrometer For Infra-Red Exploration* (MOSFIRE) at the Keck Observatory on Hawai'i. Taken together, all these instruments provide unprecedented constraints on the

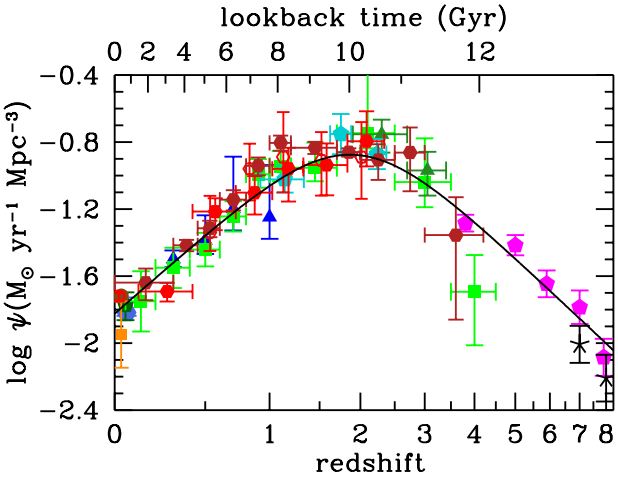

Figure 1.6: The cosmic star formation rate density (SFRD, ψ; per comoving volume) as a function of redshift and lookback time (shown on the bottom and top abscissa, respectively). The coloured points show measurements from different surveys and the solid line shows the best-fit. The SFRD increases with time up to a broad peak roughly 10 billion years ago, followed by a factor ≈ 8 decrease towards the present day. *Figure taken from Madau & Dickinson (2014).*

SED of distant galaxies in the HUDF and work towards an integrated view of their physical properties.

1.4 The state of the art

1.4.1 Star formation in galaxies across cosmic time

Observations of star-forming galaxies have revealed how the cosmic star formation rate density (SFRD) evolves with time in increasing detail (e.g., Lilly et al., 1996; Madau et al., 1996; Hopkins & Beacom, 2006; Madau & Dickinson, 2014), out to when universe was only a few hundred million years old (e.g., Bouwens et al., 2015). The SFRD is shown in Figure 1.6. From the formation of the first galaxies at *cosmic dawn*, the SFRD of the universe has increased with time, up to a broad peak around 10 billion years ago (between redshift $1 - 3$), often referred to as *cosmic noon*. Since then, it has declined by a factor ≈ 8 towards the present day. The detailed evolution of the SFRD beyond the peak (towards the earliest times) is uncertain, however, in particular because of the difficulty in constraining the amount of dust-obscured star formation (e.g., Casey et al., 2018; Bouwens et al., 2020). Explaining what drives the drives the evolution in the average star formation rate of galaxies is one of the defining features of a successful theory of galaxy formation. In theoretical work, using large computer simulations, the increase at high redshift is limited by the build-up of dark matter halos, while the subsequent evolution is driven by the balance between in- and outflows of gas

and star formation (e.g., Schaye et al., 2010) and the effectiveness of each of these processes as a function of the halo mass (e.g. Behroozi et al., 2013b). At the same time, theory predicts that, due to self-regulation, the evolution of the SFRD is relatively insensitive to the details of the star formation efficiency (or gas consumption time scale; Schaye et al. 2010; Behroozi et al. 2013a; Somerville et al. 2015). To some extent, the SFRD by itself is therefore a limited probe to understand the details of the process of star formation inside galaxies. However, by comparing the (evolution of the) cosmic SFRD to the other baryonic components, such as the cosmic atomic and molecular gas densities, it does provide insight into where the baryons reside over cosmic time, the baryon cycle of galaxies, and the global process of star- and galaxy formation. For example, were galaxies more efficient in converting their cold ISM into stars 10 billion years ago, or were they simply more cold gas-rich?

The individual star-forming galaxies (that make up the SFRD) are observed to follow a broad correlation between their stellar mass and (recent) star formation rate (Brinchmann et al., 2004; Noeske et al., 2007a), see Figure 2.7 and Figure 3.10. This relation has become known as the *main sequence of star-forming galaxies*.[11] Galaxies with a significantly higher SFR than the population average at fixed stellar mass are called *starburst galaxies*, while (massive) galaxies with relatively little star formation are considered to be *quenched*. The physical processes that drive the shape of the relation, the scatter around it, and its evolution with time, hold valuable clues about galaxy formation. While the shape and scatter are still an active topic of study (see chapter 2), it is clear that the normalisation of the relation increases out to $z \approx 3$ (e.g., Whitaker et al., 2014; Schreiber et al., 2015; Tomczak et al., 2016), in line with the cosmic SFRD. The present and future evolution of a galaxy in this parameter space is necessarily linked to the availability of cold gas to fuel the star formation, as surveys in the local universe have demonstrated (e.g., Saintonge et al., 2016, 2017). To understand this interplay over cosmic time in detail, surveys of the cold molecular gas content of galaxies with average star formation rates for their stellar mass—galaxies 'on the main sequence'—are required.

1.4.2 Molecular gas in distant galaxies

There is a long history of molecular gas observations in distant galaxies. Given the fundamental importance of molecular gas for star formation, however, it has remained surprisingly difficult to study in distant galaxies. Advances in the field have continuously been driven by the availability of more sensitive (sub)millimeter instruments, in particular interferometers.

Ever since the first detection of CO in a high-redshift galaxy, the $z = 2.28$ quasar *IRAS* F10214+4724 (Brown & vanden Bout, 1991; Solomon et al., 1992a), the number of CO

[11] The name resembles the *main sequence* of stars in the Hertzsprung-Russell diagram that are powered by nuclear fusion of hydrogen and form a tight locus along which they evolve in equilibrium. However, the relation between the SFR of galaxies and its integral over time (the stellar mass that has been built-up) is not equally straightforward. It is perhaps best considered as a cross-sectional snapshot of the population at a specific time, in which each galaxy evolves along its own star formation history (which can vary on both short and long timescales), and care should thus be expressed when interpreting its parameters (e.g., Abramson et al. 2016; Matthee & Schaye 2019, see also the recent discussion in Förster Schreiber & Wuyts 2020). In chapter 2, that deals specifically with this topic, we therefore avoid this connotation and consequently refer to the 'stellar mass – star formation rate relation'. In later chapters, however, we will use the now commonly adopted and brief term '(galaxy) main sequence'.

detections in distant galaxies has been steadily increasing. By the time of the review by Solomon & Vanden Bout (2005), a few dozen detections of CO were made in galaxies at $z > 1$. Most of these galaxies were first identified as strong emitters at far-infrared/submillimeter wavelengths, with high far-IR luminosities (greater than 10^{12} $L_\odot$). These were selected either directly from submillimeter surveys, or by following up radio galaxies or large optical surveys of high-redshift quasars. Key to the detection of CO in these sources was prior knowledge of their redshift from optical spectroscopy, because of the narrow bandwidth of the (sub)millimeter instruments. As more sensitive (sub)millimeter interferometers became available in the following decade, large reservoirs of cold gas as were confirmed in an increasing number of galaxies. Importantly, these instruments also enabled the first studies of optically-selected star-forming galaxies at $z > 1$. The total number of CO detections in distant galaxies increased to close to 200 by the review of Carilli & Walter (2013). Since then there have been major developments in the field. In particular ALMA, with its unparalleled sensitivity and angular resolution, has greatly improved our view of the molecular gas content of distant galaxies.

Submillimeter-selected galaxies (SMGs; Smail et al. 1997; Blain et al. 2002) have been among the prime targets for cold-gas observations as their high dust luminosities are indicative of large amounts of gas and dust. Observing their CO emission has been challenging, however, as the large dust attenuation often causes them to be extremely faint at optical wavelengths, making redshift determinations challenging (even to date, e.g., Danielson et al., 2017). In addition, the low angular resolution ($\geq 15''$) of the single-dish telescopes with which they were initially selected, as well as later far-IR instruments such as *Herschel*, gave rise to significant source blending and challenges in identifying the counterparts of the SMGs at other wavelengths. As such, understanding the nature of SMGs and their relation to the overall population of star-forming galaxies has been challenging. The field is now rapidly developing with ALMA (see Hodge & da Cunha, 2020, for a review). Recent studies confirm that SMGs are mostly massive and highly star-forming galaxies ($M_* \sim 10^{11}$ $M_\odot$ with SFR between 10^2 and 10^3 $M_\odot$ yr^{-1}), with most of the submm emission arising in a compact (starburst) region (though they may still host more extended disks). While SMGs have been portrayed as the high-redshift analogues of (U)LIRGS,[12] and as such the starburst outliers of the galaxy population, this picture is debatable, and SMGs are likely a diverse population of objects. While the brightest sources are linked to extreme galaxies, the boundary between faint SMGs and massive, optically-selected, star-forming galaxies is starting to fade[13] with sensitive submm telescopes (Hodge & da Cunha, 2020). SMGs generally host large reservoirs of cold gas (see Carilli & Walter, 2013, for a review), though their precise gas mass is uncertain because of the difficulty in constraining the α_{CO} (which is commonly assumed to be low, (U)LIRG like). The diversity among SMGs is also seen in their gas conditions, as reflected by the variety in their CO excitation ladders. These imply SMGs have dense and warm gas in comparison to local star-forming galaxies (Danielson et al., 2011; Bothwell et al., 2013; Birkin

[12](Ultra) Luminous Infrared Galaxies in the local universe with high infrared luminosities above (10^{12}) 10^{11} $L_\odot$, that predominantly host (merger-driven) starbursts and/or an AGN, and make up a very small fraction of the overall galaxy population (Sanders & Mirabel, 1996).

[13]Note that the average (main-sequence) galaxy with a stellar mass of 5×10^{10} $M_\odot$ is in fact a LIRG by $z \approx 1$ and a ULIRG at $z \approx 3$.

et al., 2020), although, given their diverse nature, an average CO ladder that applies to 'all' SMGs is not to be expected (Casey et al., 2014).

The first studies of optically-selected star-forming galaxies showed that they were surprisingly gas rich (Daddi et al., 2010a; Tacconi et al., 2010; Riechers et al., 2010; Tacconi et al., 2013), with fairly large reservoirs of warm gas compared to local spiral galaxies (Daddi et al., 2015). These galaxies were typically selected to be 'less extreme' than SMGs in terms of their SFR, though to enable detections, most were still selected to be massive (with M_* around 10^{10} to 10^{11} $M_\odot$) and highly star-forming (SFRs of 10 to 100 $M_\odot$ yr^{-1}), with IR luminosities in excess of 10^{11} $L_\odot$, though morphologically disk-like (e.g., Daddi et al., 2010a; Tacconi et al., 2013). These results indicated that the average cold gas fraction of star-forming galaxies at $z = 2$ is several times higher than in the local universe, and increases out to at least $z = 3$, while the depletion time decreases mildly over the same time (Tacconi et al., 2010; Geach et al., 2011; Tacconi et al., 2013), though it may show potential differences between disk-like galaxies and nuclear starburst (e.g., Daddi et al., 2010a; Genzel et al., 2010, albeit degenerate with the assumptions for α_{CO}). Large (literature) studies are now trying to constrain the evolution of the scaling relations of molecular gas fraction (f_{gas}) and depletion time (t_{depl}) (Genzel et al., 2015; Tacconi et al., 2018, 2020), and simultaneous efforts take place to constrain these from the dust-continuum emission (e.g., Scoville et al., 2017; Liu et al., 2019). Still, significant uncertainties persist in these scaling relations. Besides challenges in deriving stellar masses and SFRs for a variety of sources in a consistent and accurate way (for example, highly obscured sources such as SMGs), and biases that arise when combining large-but-incomplete samples of galaxies, there are still fundamental uncertainties in deriving gas masses for galaxies at high redshift, due to the limited knowledge about the conditions in the ISM, which drive the conversion factors. Again, submm interferometers like ALMA are now enabling progress on this front, as (larger samples of) massive star-forming galaxies can be studied in multiple tracers (in particular from CO and [C I], e.g., Popping et al., 2017b; Bourne et al., 2019; Brisbin et al., 2019; Valentino et al., 2018; Valentino et al., 2020a,b, see chapter 4).

While not strictly dealing with the cold molecular gas, this brief review would not be complete without mentioning the impact of ALMA by its ability of observing the fine-structure lines in the highest-redshift galaxies, in particular [C II] λ158 μm. While only the brightest and most extreme sources were previously observable at $z \geq 5$, massive star-forming galaxies at these redshifts can be detected in half an hour with ALMA, making it one of the prime tools for searching and spectroscopically confirming high-z galaxies. This is sparking studies of the galaxy population at $z = 5 - 6$ (e.g., Capak et al., 2015; Le Fèvre et al., 2020), spectral scan surveys for galaxies at $z = 6 - 8$ (e.g., Smit et al., 2018), and has led to the highest spectroscopic redshift to date at $z = 9.1$ (Hashimoto et al., 2018, via [O III] λ88 μm). ALMA also enables more systematic studies of the highest redshift quasars, and their companions, at sub-kpc resolution (e.g., Decarli et al., 2017, 2018; Venemans et al., 2018, 2019)

1.4.3 The need for molecular deep fields

What becomes clear from § 1.4.2 is that a significant limitation in our knowledge of the cold gas content of galaxies comes from the fact that most observations have been restricted to targets that were preselected based on their UV–FIR emission (cf. Carilli & Walter 2013).

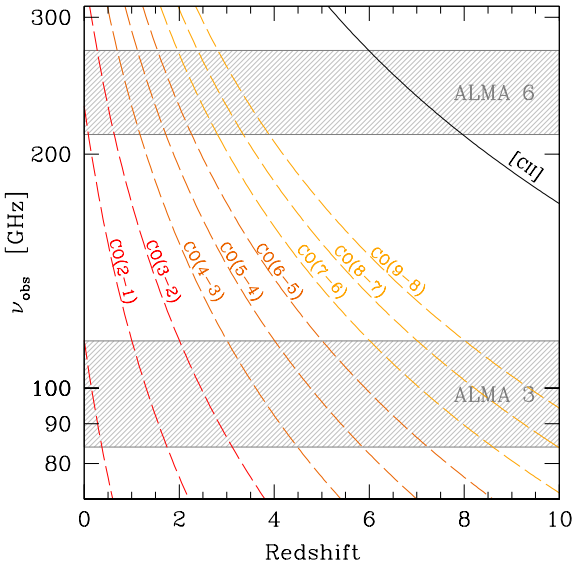

Figure 1.7: The observed frequency of the rotational transitions of carbon monoxide (up to CO $J = 9 \rightarrow 8$) as they shift with increasing redshift. The ASPECS tunings, scanning through the entire ALMA bands 3 and 6, provide almost continuous coverage of the CO signal, out to high redshift (there is only a tiny gap between $0.6309 < z < 0.6950$). Also indicated is the [C II] $\lambda 158\,\mu$m line. The transitions from atomic carbon, topic of chapter 4, follow tracks close to CO $J = 4 \rightarrow 3$ and CO $J = 7 \rightarrow 6$. See Figure 3.1 and Figure 4.1 for an alternative presentation. *Figure taken from Walter et al. (2016).*

While this approach is efficient, it leaves the possibility that a significant fraction of the molecular gas is missed, because it is not associated with the galaxies that are *a priori* expected to be most gas rich. In order to obtain a more complete picture of the molecular gas content of distant star-forming galaxies, and to perform a census of the cosmic molecular gas content of the universe, an untargeted survey for the molecular gas signal throughout cosmic time is needed. Such a survey should be sensitive enough to detect the molecular gas in the average population of star-forming galaxies. ALMA is the only telescope with sufficient sensitivity to perform such a study continuously over the past 12 billion years cosmic history, as shown by several pilot programs (Walter et al., 2014, 2016, see also Riechers et al. 2019).

1.5 The ALMA Spectroscopic Survey of the HUDF

1.5.1 Motivation

The ALMA Spectroscopic Survey of the *Hubble* Ultra Deep Field (ASPECS) is a three dimensional survey for the emission from cold gas and dust throughout cosmic time. It is the first extragalactic Large Programme approved for ALMA, totaling 150 h of observations, lead by Principal Investigators (PIs): F. Walter, M. Aravena, and C. Carilli. The primary

goal of ASPECS is to survey the cosmic molecular gas content of galaxies—the fuel for star formation—without performing any target preselection. In this way, ASPECS measures the cosmic molecular gas density, which is the necessary complement to the cosmic SFR density (SFRD) and an important missing piece in our picture of the baryon cycle.

1.5.2 Observing strategy

The ASPECS observations are specifically designed to detect emission from cold molecular gas in a well defined cosmic volume (that is, an area on the sky times a distance along the line of sight) and obtain a census of the cosmic molecular density through time, $\rho_{H_2}(z)$. This goal is achieved by imaging a significant area on the sky in a mosaic of individual ALMA images, while at the same time scanning for emission from the bright lines of CO in frequency space, down to a predetermined sensitivity limit. The transitions between the higher rotational levels of CO lie at distinct frequencies (§ 1.2.2), which redshift through frequency space as galaxies are more distant. The *spectral scans* of ASPECS are chosen such that they encompass almost the complete atmospheric transmission windows at 3 mm (from 84 to 115 GHz; band 3) and 1.2 mm (from 212 to 272 GHz; band 6). Because the effective bandwidth of ALMA is (only) 4×1.875 GHz, five frequency tunings in band 3 and eight tunings in band 6 are needed to scan through the whole spectral range (Walter et al., 2016). The result is that ASPECS can detect emission from CO at essentially all redshifts, as shown in Figure 1.7. At the same time, the spectral scans are sensitive to any other transition that falls within the frequency coverage, such as [C II] for galaxies at $6 \leq z \leq 8$ and emission from [C I] at lower redshifts, as well as fainter emission (for example, from H_2O).

The field of choice for ASPECS is the *Hubble* Ultra Deep Field, which is ideally located on the sky for observations with ALMA (at $-27°$ declination). The HUDF has been studied extensively with telescopes across the electromagnetic spectrum, providing excellent quality ancillary data both in depth and resolution. It will also be one of the prime targets for guaranteed time observations with the *James Webb Space Telescope*. The wealth of multi-wavelength data provides important constraints on the properties of the galaxies, such as their stellar mass, star formation rate, and AGN activity. Conversely, the ASPECS data greatly adds to the legacy value of the HUDF. The HUDF has also been an important target for MUSE (§ 1.3.1), which provides spectroscopic redshifts for more than 1500 galaxies in the field. This redshift information is particularly important, as it can be used to both identify the molecular gas emitters, as well as search for molecular gas below the formal detection threshold of ASPECS. The synergy between MUSE and ALMA is one of the main topics of this thesis.

1.5.3 Data products: two cubes and two images

The result of the ASPECS observations are a pair of three dimensional datacubes. Two axes of a cube are the location on the sky (in right ascension and declination) and the third axis is the observed frequency. The latter translates to a distance along the line of sight via the redshift, once the observed emission line has been identified. A rendering of the three dimensional datacubes from ASPECS can be seen in Figure 1.10. The bright spots correspond to emission lines from the cold molecular gas in galaxies, while the stripe(s) parallel to the frequency axis

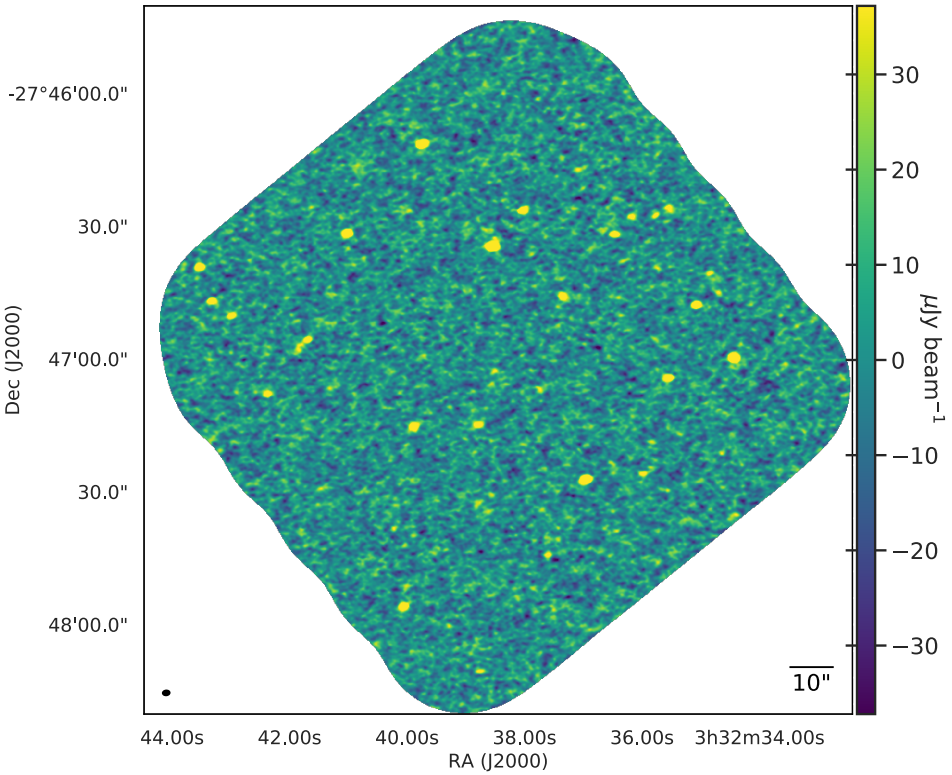

Figure 1.8: The ASPECS-LP 1.2 mm continuum map (band 6), showing the continuum emission from the cold dust in galaxies in the *Hubble* Ultra Deep Field. This map is the deepest ALMA continuum map of a cosmological deep field obtained to date, reaching a root-mean-square noise level of 9.3 μJy beam^{-1}. *The map is naturally weighted and shown down to 10% of the primary beam response (without correcting for mosaic primary beam response), which corresponds to 4.2 arcmin^2 on sky. Figure adapted from González-López et al. (2020).*

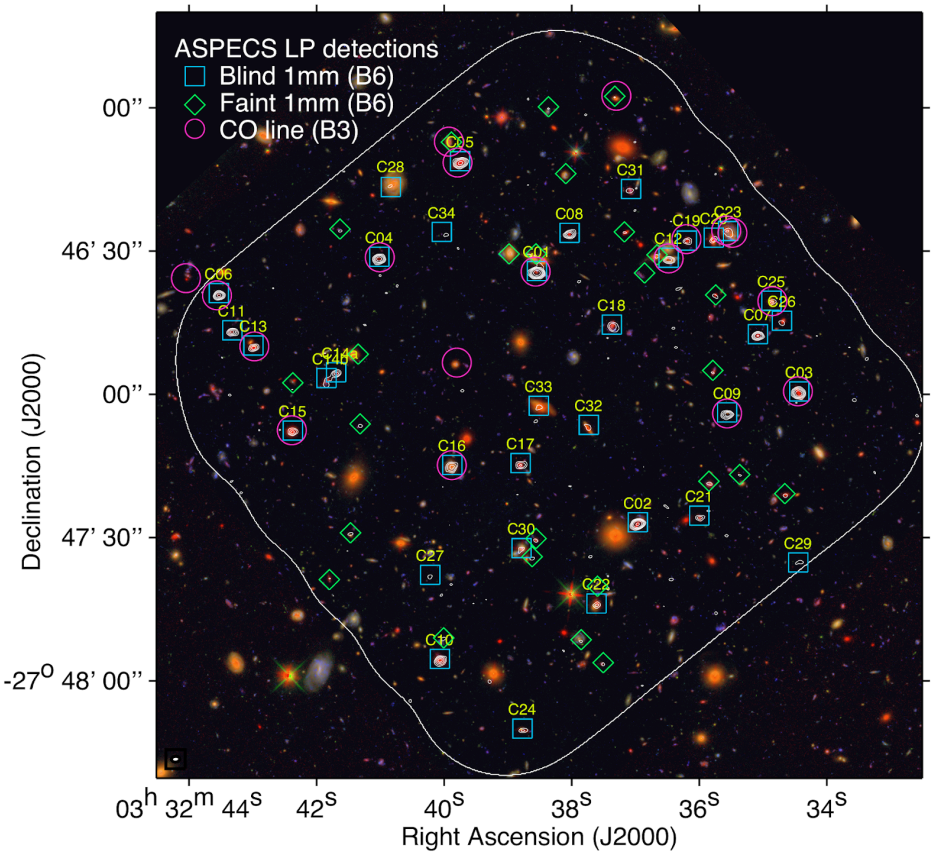

Figure 1.9: *Hubble* image of the HUDF on which we highlight the dust continuum- and CO-selected samples from ASPECS. The purple circles show the galaxies that are detected by their CO-line emission, which are the topic of chapter 3. The blue squares and green diamonds indicate the galaxies that are detected in the dust continuum (without and with a prior, respectively). The intersection between these samples, and the subsequent implication for their physical conditions, is discussed as part of chapter 4. The white contours show the ASPECS-LP 1.2 mm dust-continuum emission (cf. Figure 1.8). *Red: F160W, Green: F850LP, Blue: F450W. Contours at the 3, 5, 7, 10 and 20σ level. Figure taken from Aravena et al. (2020).*

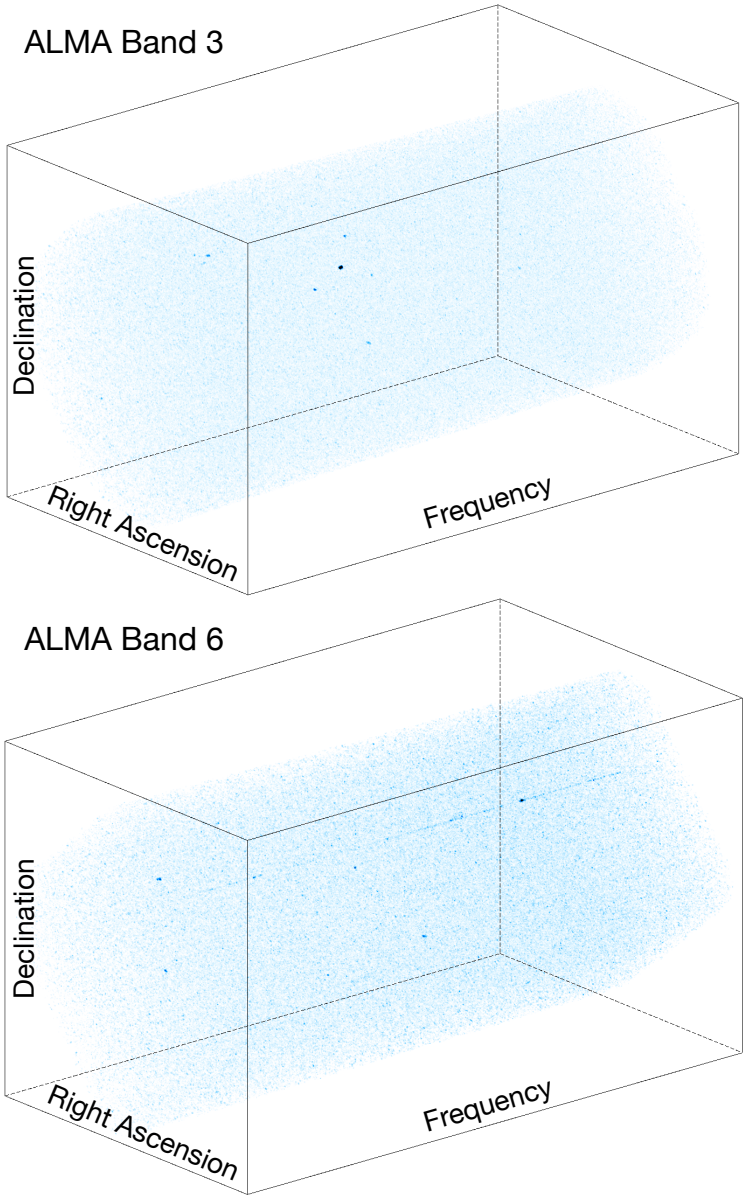

Figure 1.10: Three-dimensional rendering of the ASPECS band 3 and band 6 datacubes. The bright spots correspond to emission lines from cold gas in galaxies, while the fainter dots are increasingly due to noise fluctuations. The horizontal stripe that is clearly visible in the band 6 data is due to strong dust-continuum emission from the brightest galaxy (compare Figure 4.3). *Both renditions span about 2.′5 in the spatial directions and cover the full frequency range of the band 3 and band 6 scans.*

are due to continuum emission. The emission lines of varying brightness (including those that are not directly visible in this image) are identified through a statistical analysis of the noise.

By collapsing the cubes along the frequency axis, images of the dust continuum are obtained at the average frequency of the spectral scans. These are very sensitive, because of the sensitivity of each tuning in combination with the number of tunings, spanning a large frequency range. The band 6 image at 1.2 mm is shown in Figure 1.8 and represents one of the deepest continuum images of an extragalactic field to date.[14] The number of sources in the image that is detected above a certain sensitivity limit (the *number counts*) shows a strong flattening at the faintest levels, which implies that the observations are reaching the limits of submillimeter imaging at these frequencies, in the sense that deeper observations will not yield many additional sources. Indeed, ASPECS identifies the individual galaxies that together are responsible for almost all ($\approx$ 93%) of the *Extragalactic Background Light* at 1.2 mm in the HUDF (González-López et al., 2020; Popping et al., 2020)

1.6 The thesis

1.6.1 This thesis

This thesis presents a series of studies of the cold molecular gas in distant galaxies in the *Hubble* Ultra Deep Field. These are enabled through deep spectroscopic surveys with MUSE and ALMA, in particular ASPECS. The central question throughout these studies is: how does the cold, molecular interstellar medium of galaxies evolve over cosmic time, in relation to their star-forming properties, and how does this dictate their evolution?

The logical flow of the thesis can be understood as follows. We first study the relation between the star formation rate and stellar mass (the galaxy main sequence) in low-mass galaxies in chapter 2. We then shift focus to the cold molecular gas. We identify which galaxies are rich in molecular gas and study the conditions in their cold ISM, in relation to their star formation rate, stellar mass, and other physical properties (chapter 3 and chapter 4). We then use this information to measure the cosmic molecular gas content of the universe back in time, from the present day to when the universe was only 1.5 billion years old, and discuss how future studies can improve on these constraints (chapter 5 and chapter 6).

Chapter 2: In the hierarchical framework of galaxy formation, low-mass galaxies play a fundamental role. However, studies of the main sequence have been limited to more massive galaxies. In this initial chapter, we use MUSE to study the low-mass end of the stellar mass–star formation rate relation, a poorly sampled part of parameter space, for a flux-limited sample of galaxies in the HUDF. We use robust, dust extinction-corrected, Balmer line-derived star formation rates and apply a novel, Bayesian statistical model that jointly constrains the intrinsic scatter. We find an increased intrinsic scatter, which may signal increasingly stochastic star formation histories in low-mass galaxies, and discuss why

[14] It is at least a factor 4 deeper than other deep field surveys with ALMA, that often consist of 1.2 mm dust continuum imaging in a single frequency tuning over a larger area of the sky (e.g., Kohno et al., 2016; Dunlop et al., 2017; González-López et al., 2017a,b; Franco et al., 2018; Hatsukade et al., 2018), see also Hodge & da Cunha (2020).

previous work may have underestimated the scatter. We also find a flatter slope than predicted by simulations, which suggests that the modeling of feedback processes in low-mass halos is still to be improved.

Chapter 3 answers perhaps the most simple question one can ask when doing a survey like ASPECS: what is the nature and what are the physical properties of the galaxies we detect in a flux-limited survey for molecular gas as traced by CO? We identify all the emission lines as redshifted CO, arising from the cold molecular gas in galaxies that are visible to *Hubble*. Using the MUSE spectra, we measure that the gas in galaxies at $z \leq 1.5$ has a solar metallicity, which supports the use of a Galactic conversion factor ($\alpha_{\rm CO}$) to measure their molecular gas mass. The results show that ASPECS unveils the molecular gas in the majority of the massive, star-forming galaxies at cosmic noon. The low SFR of some detected galaxies, however, highlights that previous, star formation-based selection methods can miss part of the gaseous galaxy population.

Chapter 4 studies the physical conditions in the ISM of the ASPECS-detected galaxies, by means of their CO excitation, atomic carbon emission, and dust-continuum emission. Combining the ALMA observations with those from the VLA, we measure and predict (using theoretical models) the average low-, mid- and high-J excitation for the galaxies observed with ASPECS. Focusing on the results from CO, we find that the excitation, and thus the average density and temperature in the cold ISM, increases with redshift. At the same time, the ASPECS galaxies show less excited CO ladders than earlier samples of optically- and submillimeter-selected galaxies at comparable redshifts. Both phenomena can be explained by the (lower) star formation rate surface densities of our galaxies (compared to earlier surveys).

Chapter 5: Building on the foundation laid out in chapters 3 and 4, all aspects come together in this chapter, where an inventory and a statistical analysis of the multi-line signal in the ASPECS data is performed. We combine the necessary redshift and metallicity information (chapter 3) together with knowledge we obtained about the CO excitation and the conditions in the ISM (chapter 4) to construct the cosmic molecular gas density, $\rho_{\rm H_2}(z)$. The main result is that $\rho_{\rm H_2}(z)$ increases with cosmic time, up to a peak at $z \sim 1.5$, followed by a drop towards the present day, in agreement with the evolution of the cosmic star formation rate density. This implies that the rise and fall of the cosmic star formation rate density is indeed linked to the increased gas content of galaxies at cosmic noon, and that the molecular gas depletion time in galaxies is approximately constant with redshift, after averaging over the galaxy population.

Chapter 6: In this final chapter ASPECS is pushed one step further. Starting from the large number of Lyα-redshifts from MUSE, we determine the systemic redshifts of $z = 3 - 4$ galaxies from other spectral features at restframe UV and optical wavelengths, through near-IR spectroscopy. Using the exact distance information, we stack the molecular gas and dust signal in these low-mass galaxies, observed when the universe was only ~ 2 Gyr old. We show that the molecular gas and dust is very hard to detect, because the metallicity in the ISM of these galaxies is significantly sub-solar, as it is still being enriched with metals. We conclude by pointing in future directions that could be taken to measure the cold gas reservoirs in these galaxies.

1.6.2 Related science with ASPECS

The ASPECS observations enable a wide range of science beyond what is presented in the following chapters. This is reflected in the well over a dozen publications from the ASPECS team, as well as others that have used the pubicly available data.[15] Here we briefly summarise some of these studies, in relation to this thesis, in particular those that are not discussed in as much detail in the following chapters.

Aravena et al. (2019) discuss the evolution of the molecular gas content and star-forming properties of the CO-selected ASPECS galaxies (studied in chapter 3 and chapter 4), in the broader context of the galaxy scaling relations between molecular gas factions, depletion times, and distance from the galaxy main sequence. Most galaxies from the flux-limited sample follow the relations (to within uncertainties), although there is some tension with galaxies that would be missed by earlier (targeted) observations (see also chapter 3). A follow-up study of the dust continuum-selected sample is presented in Aravena et al. (2020). Both studies conclude that galaxies with an average star formation rate are the dominant contributors to the overall molecular gas density. Figure 1.9 provides an overview of the HUDF galaxies that are detected through their low-J CO and/or 1.2 mm dust-continuum emission.

Inami et al. (2020) leverage the MUSE redshifts to study CO emission below the formal detection threshold of ASPECS (see also chapter 3) and perform a CO-stacking study to constrain the molecular gas content of galaxies up to $z = 3$ (stacking results at $z \geq 3$, where MUSE alone is insufficient, are discussed in chapter 6). They detect CO in individually undetected galaxies at $z \sim 1.5$ and place constrains on the gas fractions of galaxies towards lower stellar masses. They find limited additional signal at higher redshift, in good agreement with the ASPECS intensity mapping study from Uzgil et al. (2019).

Magnelli et al. (2020) study the evolution of the cosmic densities of dust and molecular gas as a function of time, through a dust continuum-stacking analysis of all H-band selected galaxies in the HUDF. They find an early rise, peak at $z \sim 2$, and decline towards the present, similar to the cosmic SFRD, and consistent with the result from chapter 5. Their results imply that by a large fraction ($\sim$ 90%) of the dust formed in galaxies across cosmic time has either been destroyed or ejected into the intergalactic medium by $z = 0$.

Bouwens et al. (2020) study the obscured star formation of distant (Lyman break-selected) galaxies, out to the first 500 million years of cosmic time ($z = 10$). Updating constraints on the correlation between the dust extinction and re-emission in the IR (the IRX–β-relation), they refine the estimates of the cosmic SFRD at $z > 3$ and show how relative fraction of obscured versus unobscured star formation evolves as a function of cosmic time.

Kaasinen et al. (2020) perform a detailed study of three ASPECS galaxies at higher resolution, comparing the spatial extent of their CO, dust, and (rest-frame optical) stellar emission. They find a variety of morphologies, with both compact and extended ISM distributions (despite similar selection criteria), and emphasise the importance of surveys that are not biased to submm bright sources, which are more likely to show compact dust emission.

[15] https://www.aspecs.info

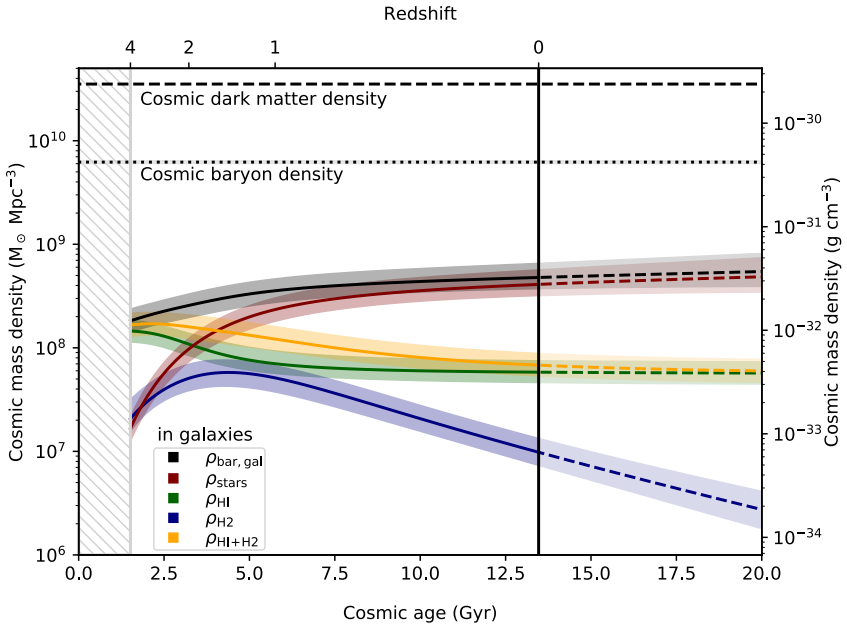

Figure 1.11: The evolution, as a function of cosmic time, of the cosmic mass densities of: stars (red, cf. Figure 1.6), neutral hydrogen (H I, green, as derived by Walter et al., 2020), and molecular gas, H_2, as derived by ASPECS (blue). The latter is the topic of this thesis and is discussed extensively in chapter 5 and is shown in Figure 5.9. Also shown are the the sum of the gaseous components (yellow, H I + H_2) and the sum of all the baryons (grey, the sum of all curves), and the cosmic baryon and dark matter densities (dotted and dashed lines, respectively). The lower abscissa indicates the cosmic age of the universe and the upper abscissa the corresponding redshift. The figure starts 1.5 Gyr after the big bang (at redshift $z = 4$) and shows the measured evolution towards the present day ($z = 0$). The dashed segments are a hypothetical extrapolation into the future, under the assumption of continuity and that the current physical processes continue to dominate. *Figure taken from Walter et al. (2020).*

1.7 The future

1.7.1 The cosmic baryon cycle

The evolution of the cosmic molecular gas density, as measured in chapter 5, can be combined with the evolution of the cosmic densities of stellar mass, star formation rate, and neutral gas to constrain the evolution of the baryons associated with galaxies, averaged over space and time. This analysis is presented in Walter et al. (2020) and briefly summarised here. Figure 1.11 shows the evolution of the cosmic mass densities. The cosmic density of H I has slowly declined over the past 12 billion years (cf. Neeleman et al., 2016), while the density of H_2 increases and decreases, similar to the evolution of the SFR (chapter 5). Significant accretion of gas onto galaxies is required in order to sustain the star formation needed to form

the bulk of the stellar mass seen in galaxies in the last 9 billion years. The relative evolution of the atomic and molecular mass densities can be explained via a two-phase accretion process: (i) the inflow of diffuse (ionised) gas into the (extended) H I reservoir of a galaxy and (ii) the subsequent inflow of atomic gas towards the centre of the potential well, the conversion to molecular gas, and the formation of stars. This is in line with the observation that the star formation rate surface density in galaxies is correlated with the molecular gas density (§ 1.2.2). The cosmic star formation rate density is then driven by the net availability of molecular gas, as it is (indirectly) accreted onto galaxies. A comparison to numerical simulations suggest that the decreased gas accretion rates in the last 9 billion years are the result of the decreased growth of dark matter halos (partly due to the expansion of the universe), combined with the effects of feedback from stars and accreting black holes. Extrapolating the evolution of the mass densities into the hypothetical future paints a picture in which the molecular gas density continues to decline, with limited growth in the stellar mass density, as the cosmic star formation rate density steadily diminishes.

1.7.2 Science and facilities

Because of its unparalleled scale and sensitivity, ALMA will continue to play a central role in the study of cold gas in distant galaxies (and submm science in general) in the years to come. It is not even at its full potential: certain aspects of the observatory are still being completed and further technological developments are marked on the ALMA roadmap (Carpenter et al., 2019) that improve the sensitivity, frequency coverage, bandwidth and angular resolution of the instrument. Particularly relevant are the planned Band 1 and 2 receivers, that will enable the observations of CO $J = 1 \rightarrow 0$ in galaxies up to $z = 2$, removing the need for the uncertain excitation corrections—that play a central role in this thesis—and anchor $\rho_{\mathrm{H_2}}$ even more firmly. Increasing the bandwidth for ALMA is another important avenue—ideally to cover the entire atmospheric transmission windows all at once. This will allow for much greater efficiency of spectral scan surveys, which are becoming increasingly popular (note three of the four large programs in the "Cosmology and High Redshift Universe" Science Category to date are spectral scans[16]). At the same time, this will greatly increase the continuum sensitivity, which will also help reduce the increasing demand in the total observing time. These improvements will allow an increasing investment in large(r) programs, which are instrumental for the study of distant galaxies. Indeed, in light of the monumental time investments of the great observatories in the extragalactic deep fields, the ASPECS program should not be seen as the end point, but only as the beginning.

Future studies of cold gas in distant galaxies, with a range of different submm facilities, should focus on different aspects to advance our insight into the process of galaxy assembly. In addition to spectral scan surveys (mentioned above), and studies of larger samples in single, well-calibrated tracers, targeted multi-line studies will provide insight into the cold ISM conditions and should (eventually) aim at mapping the 'complete' (sub)mm spectra of different classes of galaxies. At the same time, while expensive in terms of observation time, higher

[16] Besides ASPECS and ALPINE (The ALMA Large Program to INvestigate [C II] at Early Times, PI: Olivier Lé Fevre; which is not a spectral scan survey), these are the ALMA Lensing Cluster Survey (PI: K. Kohno) and the Reionization Era Bright Emission Line Survey, REBELS (PI: R. Bouwens).

resolution observations of both the dust and gas (kinematics) of larger samples of galaxies are much-needed, to peer into the cold ISM of distant galaxies and probe the interplay between stars, gas and dust, and the physics of star formation at smaller scales.

Finally, several new windows on distant galaxies will be provided in the near future through instrumental advances across the electromagnetic spectrum. Two facilities that are particularly relevant are the *James Webb Space Telescope* and the *Extremely Large Telescope*. Together, these will provide much-needed advances in terms of spatial resolution, sensitivity and wavelength coverage, to study the stellar populations, the build-up of dust and metals, and the (co)evolution galaxies and their supermassive black holes in distant galaxies.